Regular Article
pISSN: 2288-9744, eISSN: 2288-9752
Journal of Forest and Environmental Science
Vol. 40, No. 1, pp. 15-23, March, 2024
https://doi.org/10.7747/JFES.2024.40.1.15

JFES
Journal of Forest and Environmental Science

Accuracy Assessment of Forest Degradation Detection in Semantic Segmentation based Deep Learning Models with Time-series Satellite Imagery

Woo-Dam Sim and Jung-Soo Lee*
Division of Forest Sciences, Department of Forest Management, College of Forest and Environmental Sciences, Kangwon National University, Chuncheon 24341, Republic of Korea

Abstract

This research aimed to assess the possibility of detecting forest degradation using time-series satellite imagery and three different deep learning-based change detection techniques. The dataset used for the deep learning models was composed of two sets, one based on surface reflectance (SR) spectral information from satellite imagery, combined with Texture Information (GLCM; Gray-Level Co-occurrence Matrix) and terrain information. The deep learning models employed for land cover change detection included image differencing using the Unet semantic segmentation model, multi-encoder Unet model, and multi-encoder Unet++ model. The study found that there was no significant difference in accuracy between the deep learning models for forest degradation detection. Both training and validation accuracies were approximately 89% and 92%, respectively. Among the three deep learning models, the multi-encoder Unet model showed the most efficient analysis time and comparable accuracy. Moreover, models that incorporated both texture and gradient information in addition to spectral information were found to have a higher classification accuracy compared to models that used only spectral information. Overall, the accuracy of forest degradation extraction was outstanding, achieving 98%.

Key Words: deep learning, forest degradation, unet, GLCM, remote sensing

Introduction

Remote sensing technology has been widely adopted in the forestry sector due to its ability to monitor large-scale areas periodically, despite the difficulty of accessibility. There is currently a growing interest in the forestry regarding the upcoming launch of agricultural and forestry satellites, which has led to increased attention on the utilization of satellite technology in conjunction with the Fourth Industrial Revolution. The Korea Forest Service aims to integrate Fourth Industrial Revolution technologies with forestry R&D research through the K-Forest initiative. One of the proposed strategies is to introduce digital and contactless technologies into the forestry sector (Korea Forest Service 2024). Remote sensing technology is a representative method of digital and contactless technologies. This technology is advantageous in analyzing areas that are difficult to access or large-scale regions. It is expected to play a

Received: February 19, 2024. Revised: February 29, 2024. Accepted: March 2, 2024.

Corresponding author: Jung-Soo Lee
Division of Forest Sciences, Department of Forest Management, College of Forest and Environmental Sciences, Kangwon National University, Chuncheon 24341, Republic of Korea
Tel: +82-33-250-8334, Fax: +82-33-242-4484, E-mail: jslee72@kangwon.ac.kr

significant role in long-term forest change monitoring and forest management activities (Kim et al. 2019; Woo et al. 2019). According to the Korea National Institute of Forest Science's (NIFoS) second medium- to long-term technology development plan for 2021, research is underway to create ICT-based integrated digital forest management systems that will utilize agricultural and forestry satellites. These satellites are set to launch in 2025 and will be capable of producing high-resolution images that can monitor the entire country every three days. This initiative is expected to provide quick and accurate information for forest management and policy decision-making in areas such as forest change detection, disaster monitoring, and resource management (Cha et al. 2022).

The Korea Forest Service has announced its third basic plan for forest statistics. The aim is to compile forest basic statistics every year to contribute to national greenhouse gas management and develop tailored statistics for citizens. To update the forest cover map renewal cycle, they plan to utilize AI technology. This will improve the accuracy of forest basic statistics with transparency, as advocated by the IPCC. Applying Tier 3-level spatial approaches in greenhouse gas statistics reporting for climate change adaptation is effective in enhancing the accuracy of statistical information. Overall, the utilization of Fourth Industrial Revolution technologies and remote sensing technology will help to achieve these goals (Lee et al. 2016; Park et al. 2018).

In particular, the IPCC provides two spatial approaches for constructing national greenhouse gas statistics at the Approach 3 level with the Sampling method and the Wall-to-Wall method. The Sampling method involves estimating land cover areas through periodic sample surveys at regular intervals, while the Wall-to-Wall method calculates land cover areas at the spatial unit level. The Wall-to-Wall method for land cover classification uses semantic segmentation with deep learning models like U-Net, DeepLab, FCN, SegNet, and PSPNet. Studies show high performance, but limitations exist in distinguishing between land cover and land use categories due to remote sensing data (Cho et al. 2014; Solórzano et al. 2021; Son et al. 2022). Studies have been conducted to improve accuracy by comparing different deep learning models or investigating input information changes.

The objective of this study is to evaluate forest degradation using satellite imagery and deep learning models such as image differencing, multi-encoder Unet, and multi-encoder Unet++.

Materials and Methods

Study area

The study area is Chuncheon, which is the second-most populous city in the Gangwon Province of South Korea. Chuncheon covers an area of approximately 1,120 square kilometers. As per the statistics released by the Ministry of Land, Infrastructure, and Transport in 2023, forests cover approximately 75% of Chuncheon City, making it the most extensive category. Wetlands and croplands account for 9.2% and 8.9%, respectively. There have been some changes in land use since 2013. Grasslands and wetlands have remained relatively stable, while forests have decreased by 0.6% and croplands decreased by 0.5%. However, the area occupied by artificial facilities such as residential areas has increased by 1.1% (MLIT 2023).

Used data

To apply deep learning models, we used RapidEye satellite imagery from two periods (October 9, 2014, and May 21, 2018). The RapidEye imagery provides information from four bands: red, blue, green, and near infrared (NIR), along with the red edge band, making it effectively applicable for forest and crop monitoring (Kross et al. 2015). This study used level 3A imagery that underwent radiometric, sensor, and geometric corrections. Additionally, it utilized spatial information that included Digital Elevation Model (DEM) data obtained from the National Geographic Information Institute and forest management database (DB) information provided by the Korea Forest Service. The forest management DB contains spatial data on afforestation, logging, and forest plantation activities nationwide from 2015 to 2020. Lastly, to compare with the forest change map generated from the deep learning models, a spatial DB for forest degradation was constructed using cadastral maps and land cover maps.

Research method

To identify the degradation of forests, deep learning

models were developed by utilizing satellite imagery from two different time periods. Land cover maps were then created for each time series. The use of three deep learning models, i.e., Unet, multi-encoder Unet, and multi-encoder Unet++, helped in determining the forest degradation. Later, the accuracy of each deep learning model was compared and evaluated by comparing the extracted forest degradation information from cadastral maps and visual inspection with that of the deep learning models (Fig. 1).

Dataset construction for deep learning model application

In order to establish land cover classification based on semantic segmentation models, it is essential to prepare input and label images (Géron 2022). Dataset A used five spectral bands from the RapidEye satellite imagery. These bands include the green, blue, red, red-edge, and near infrared (NIR) bands. On the other hand, Dataset B combined spectral data with texture and terrain information. Specifically, texture attributes such as Homogeneity, Entropy, and Correlation were derived from the Gray-Level Co-occurrence Matrix (GLCM). The computation of texture features can be different based on various parameters such as window size, quantization level, and pixel distance, leading to diverse texture representations (Haralick et al. 1973; Clausi 2002). For this study, we computed texture attributes using a window size of 15 by 15, which corresponds to an area of approximately 0.5 hectares. Additionally, terrain information, specifically slope details, were extracted from Digital Elevation Model (DEM) data. The DEM was created using the 1:5,000 scale digital topographic maps provided by the National Geographic Information Institute. To construct land cover classification, seven classification categories were defined, including the six land use categories defined by the IPCC (forest, cropland, grassland, wetland, settlements, other land), along with forestry-managed land. The label images for the time-series deep learning model were constructed using visual interpretation of land cover types at a finer resolution, along with data from the national forest management database.

There are two types of datasets with training data and validation data. The purpose of the training data is to train the deep learning models, while the validation data is used to improve the accuracy of the model during training. The test data is then used to apply the trained models. The images in the datasets were set to a size of 256×256 pixels. To partition the input and label images, they were both divided into tiles of this size. The tiled images were created by randomly sampling approximately 10% of the study region's area using a random sampling technique. These tiles were then used in a ratio of 7:3 for the training and validation data, respectively. To combat the issue of decreased classification accuracy at the edges of images in CNN-based deep learning models, a 50% overlap was applied during the process of dividing the entire area of each administrative district into tiled images for the test data. For each period, a total of 113 training data and 47 validation data were created.

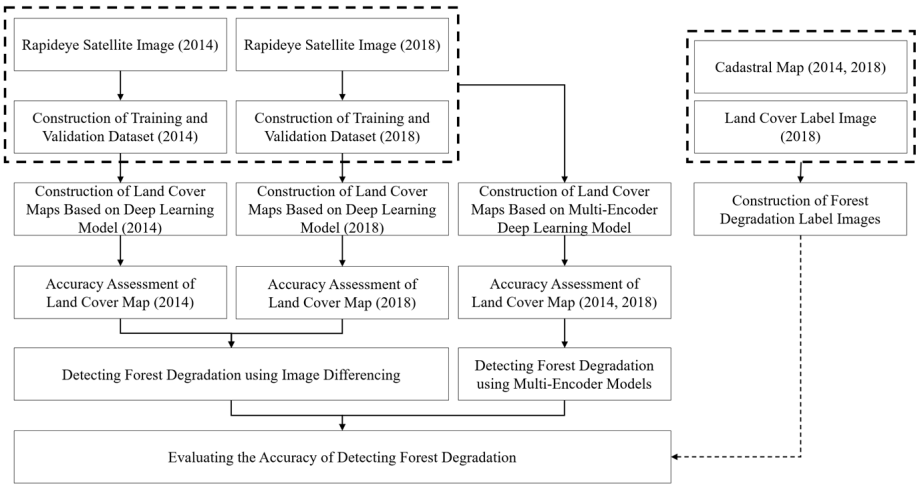

Fig. 1. Methodology for detecting forest degradation.

Construction of deep learning model algorithms

Deep learning models have been used to detect forest degradation. To evaluate the performance of land degradation detection, the Unet model along with the multi-encoder structures of Unet and Unet++ were adopted. The algorithms for forest degradation detection were categorized into two methods of image differencing technique and methods utilizing multi-encoders. The image differencing technique involved utilizing the Unet model to perform land cover classification on images from the initial and final periods and calculating the difference between them to determine the changes over time.

The Unet model is composed of encoder and decoder components. The encoder extracts feature information from the image using Unet blocks, which consist of two convolutional layers. The encoder undergoes downsampling four times in a straightforward structure. On the other hand, in the decoder, upsampling is performed four times to restore the downsized images to their original resolution. After each upsampling operation, skip connections are used to incorporate feature information from each layer of the encoder. This helps to prevent information loss and gradient vanishing issues. Although the Unet model was developed in 2015, its highly efficient structure has led to the creation of several derivative models such as ResUnet, Unet++, Attention Unet, and TransUnet, among others (Ronneberger et al. 2015; Oktay et al. 2018; Zhang et al. 2018; Zhou et al. 2018; Chen et al. 2021). The multi-encoder model is a framework that makes use of N encoders with equivalent structures in the encoder part. In this particular study, two encoders with identical structures were used. Encoder 1 takes images from the initial period, while encoder 2 takes images from the final period as input. Both encoders produce land cover maps for their respective periods simultaneously. Additionally, an embedded automation algorithm was used to calculate the difference between the land cover maps from different periods. This provides information on land degradation. Moreover, the multi-encoder model has two variations: the multi-encoder Unet model, which employs the same structure as the base model Unet, and the multi-encoder Unet++ model, which enhances the decoder and skip-connection structures. These variations were introduced to further improve the accuracy of forest degradation detection. The Unet++ model, developed by Zhou et al. (2018), is a deep learning model influenced by Densnet and features a decoder structure. It involves upsampling low-resolution feature maps and overlaying them while adding dense blocks between the encoder and decoder to learn more complex features (Fig. 2).

Setting parameters for deep learning training models

The training process of a deep learning model begins with the initialization of weights using small random values. During training, the model processes the input data through each layer, producing output. A loss function is then applied to compute the disparity between the predicted and actual values. The objective is to minimize this loss, achieved by calculating the gradient of the loss with respect to each weight and updating the weights accordingly (Rumelhart et al. 1986; Kingma and Ba 2014). This proc-

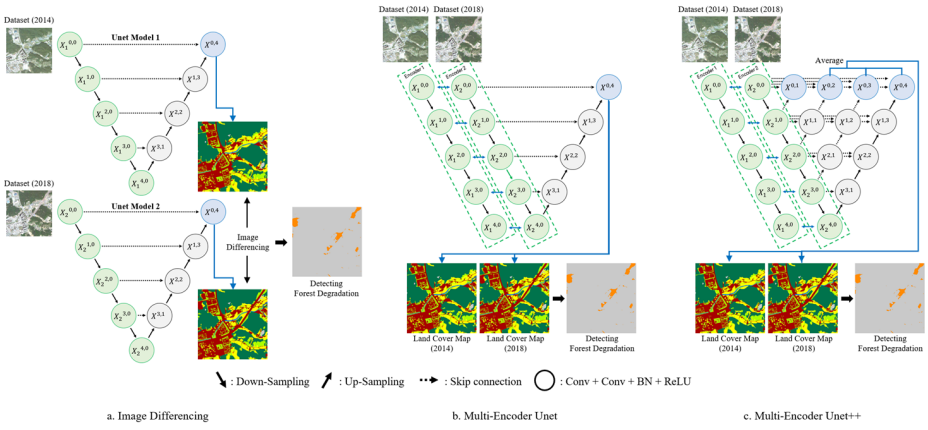

Fig. 2. The architectures of U-Net models based on image differencing technique, multi-encoder-based U-Net model, and multi-encoder based U-Net++ model.

ess iterates over a set number of epochs, adjusting weights based on both training and validation data to minimize the disparity between predicted and actual values. The learning rate, a critical parameter in deep learning, can be set using a fixed value or dynamically adjusted using techniques like learning rate scheduling. The optimizer then updates the weights based on the calculated gradients. In our study, we focused on enhancing the accuracy of the deep learning model by fine-tuning key parameters such as the loss function, learning rate scheduler, and optimizer (Loshchilov and Hutter 2018; Smith and Topin 2019). Specifically, training model utilized the cross-entropy loss function and the Adam optimizer for semantic segmentation tasks. The learning rate scheduler started at 0.01 and progressively decreased with each epoch.

Evaluation of deep learning model accuracy for land cover classification and forest degradation detection

The trained deep learning model was utilized to generate a land-cover map. The accuracy of land cover classification and forest degradation detection using deep learning was assessed by comparing these maps with labeled images. The confusion matrix was constructed by comparing labeled images with the classification map based on deep learning, and accuracy was assessed by calculating the Overall Accuracy and Kappa coefficient (Rouhi et al. 2015; Huang and Rust 2018). Additionally, precision and recall were calculated to evaluate the classification accuracy for each category, and accuracy was further assessed using the F1-score. To calculate OA, Kappa, and F1-score, the metrics True Positive (TP), True Negative (TN), False Positive (FP), and False Negative (FN) are utilized. TP refers to the instances correctly identified as positive, TN indicates instances correctly identified as negative, FP represents instances incorrectly identified as positive, and FN denotes instances incorrectly labeled as negative, serving as fundamental components in evaluating the performance of classification models by distinguishing between accurately and inaccurately classified instances.

$$\text{Overall Accuracy} = \frac{TP + TN}{TP + TN + FP + FN} \quad (1)$$

$$\text{Kappa} = \frac{OA - P_e}{1 - P_e} \quad (2)$$

$$P_e = \left(\frac{TP + FN}{TP + FN + FP + TN} \times \frac{TP + FP}{TP + FN + FP + TN}\right) + \left(\frac{FP + TN}{TP + FN + FP + TN} \times \frac{FN + TN}{TP + FN + FP + TN}\right) \quad (3)$$

$$\text{Precision} = \frac{TP}{TP + FP} \quad (4)$$

$$\text{Recall} = \frac{TP}{TP + FN} \quad (5)$$

$$F_1 - \text{Score} = \frac{2 \times Precision + Recoll}{Precision + Recall} \quad (6)$$

Result and Discussion

Distribution characteristics of deep learning training data by category

When comparing the area distribution of the deep learning training data, it was found that the forest decreased from the initial period to the final period. On the other hand, the areas of grassland, settlement, and forestry-managed land increased during the same period (Table 1).

When the surface reflectance (SR) was examined according to categories in the training data, it was found that the SR of red was highest in other lands, settlement, and croplands. On the other hand, NIR was highest in forest, grasslands, and croplands. Forest and wetland areas displayed distinct distribution characteristics compared to other categories, while cropland, settlement, and other lands exhibited similar distribution patterns due to their high

Table 1. Construction of deep learning dataset for detection of forest degradation

The number of images		Date of image acquisition	Land cover categories by area in the training data						
Training data	Validation data		Forest	Cropland	Grassland	Wetland	Settlement	Other land	Forestry-managed land
113	47	2014.10.09	66.0%	7.8%	8.5%	8.9%	5.5%	2.3%	0.9%
		2018.05.21	64.5%	7.8%	8.7%	9.4%	5.9%	1.5%	2.2%

overlap. In particular, other lands encompassed croplands and settlements and displayed a wide range of distribution characteristics. Croplands showed high overlap with settlement due to the inclusion of facility cultivation areas, leading to similar distribution patterns. Grasslands overlapped with croplands, settlements, and forests (Table 2). When the distribution characteristics of Gray-Level Co-occurrence Matrix (GLCM) were examined by category, Entropy and Homogeneity exhibited similar distribution patterns across categories. However, Correlation mostly showed negative values, indicating an opposite trend in distribution. Correlation exhibited varying distributions across land cover categories, suggesting it as the most suitable GLCM information for land cover classification. Finally, when the distribution characteristics of slopes were compared by category, forest and grasslands showed higher slope distributions. On the other hand, wetlands and croplands exhibited relatively lower slope distributions. The distribution of surface reflectance (SR) in forestry-managed lands shows that the red band had higher values in harvested areas, while NIR was more prominently distributed in planted areas. Harvested areas usually look yellow and red due to which the red band is more prevalent. On the other hand, planted areas have young trees and timber, making NIR more prevalent.

When comparing the SR characteristics among the six land use categories, harvested areas in forestry-managed land showed similarities in surface reflectance with croplands and grasslands, while planted areas in forestry-managed land exhibited similar SR distributions to forests and grasslands. The category-specific distribution patterns between the baseline and final periods were found to be similar regarding the SR distribution characteristics of the time series training data. Categories that had vegetation, such as forests, croplands, grasslands, and forestry-managed lands, showed similar spectral patterns, while categories featuring artificial structures, rocks, and bare soil, such as settlement and other lands, exhibited comparable spectral patterns. The baseline images, which were captured during non-growing seasons, displayed relatively lower average spectral values of red and NIR compared to the final period images when comparing the spectral distributions between the image acquisition periods.

Evaluation of deep learning model consistency based on training conditions

A comparison of training and validation accuracy among deep learning models for land cover classification and detecting forest degradation revealed no significant differences in accuracy between the models. The models exhibited an average training accuracy of approximately 89% and an average validation accuracy of around 92%.

Table 2. The distribution characteristics of surface reflectance in the training data by category

Period	Land cover category	Surface reflectance		GLCM			Slope
		Red	NIR	Correlation	Entropy	Homogeneity	
The base year	Forest	249±109	866±235	0.09±0.34	7.82±0.05	0.05±0.02	27.0±10.9
	Cropland	794±456	1,434±430	-0.00±0.34	7.79±0.11	0.05±0.03	4.6±4.9
	Grassland	563±315	1,172±328	-0.02±0.34	7.81±0.07	0.04±0.02	10.7±9.8
	Wetland	220±207	379±343	-0.00±0.25	7.52±0.56	0.09±0.09	0.6±3.1
	Settlement	1,051±557	1,422±511	-0.03±0.32	7.82±0.07	0.04±0.02	6.6±7.4
	Other land	1,166±622	1,524±604	0.07±0.37	7.76±0.17	0.05±0.04	15.5±14.3
	Forestry-managed land	421±195	1,079±287	0.00±0.32	7.82±0.04	0.04±0.03	25.4±9.8
Final year	Forest	260±127	3,337±659	-0.05±0.31	7.83±0.05	0.04±0.02	27.2±10.9
	Cropland	1,101±507	2,547±748	-0.03±0.34	7.80±0.09	0.05±0.03	4.8±5.0
	Grassland	690±435	3,186±761	-0.07±0.34	7.82±0.07	0.04±0.02	11.9±10.1
	Wetland	459±288	821±921	-0.01±0.30	7.53±0.59	0.08±0.09	1.3±5.3
	Settlement	1,369±664	2,632±651	-0.06±0.31	7.81±0.08	0.04±0.02	7.4±8.3
	Other land	1,690±935	2,747±910	0.02±0.37	7.77±0.18	0.05±0.04	17.0±16.2
	Forestry-managed land	640±366	3,083±823	0.01±0.35	7.82±0.06	0.04±0.02	25.6±10.0

Interestingly, the validation accuracy was about 3% higher than the training accuracy for forest degradation detection models. When the training accuracy surpasses the validation accuracy, it typically raises concerns about overfitting. However, in this study, the higher validation accuracy, coupled with stable distribution values of loss, suggests that overfitting was not a significant issue (Table 3). Regarding the comparison of training times across different deep learning models, the image differencing method had the shortest training time. However, it only learns from data from a single period, which may not be suitable for considering both initial and final periods. On the other hand, the multi-encoder Unet model was deemed to be cost-effective and efficient when considering the training processes for both initial and final periods. The multi-encoder Unet++ model did not significantly improve accuracy compared to the image differencing method and the multi-encoder Unet model. Moreover, its training time was over 2.5 times longer than that of the multi-encoder Unet model, indicating lower efficiency.

Based on the evaluation of accuracy between land cover classification maps generated by different deep learning models and the land cover classification labels (validation data), it was found that the image differencing method using Dataset B achieved the highest Overall Accuracy (OA) and Kappa statistics. We observed that including texture and terrain information, along with spectral information, improved classification accuracy across all models (Fig. 3,

Table 3. Evaluate the accuracy of deep learning models for each type of dataset

Deep learning model	Period	Dataset	Training data		Validation data		Training time (minutes)
			Accuracy	Loss	Accuracy	Loss	
Image differencing	The base year	A	89.6%	1.31	92.5%	1.25	119.7
		B	89.6%	1.32	92.8%	1.25	138.3
	Final year	A	89.1%	1.31	90.1%	1.24	120.6
		B	90.1%	1.30	91.5%	1.25	141.9
Multi-encoder Unet	The base year & final year	A	88.7%	1.31	92.4%	1.25	196.5
		B	88.7%	1.32	92.3%	1.24	220.2
Multi-encoder Unet++	The base year & final year	A	89.4%	1.32	92.4%	1.24	486.9
		B	89.3%	1.31	92.3%	1.24	556.8

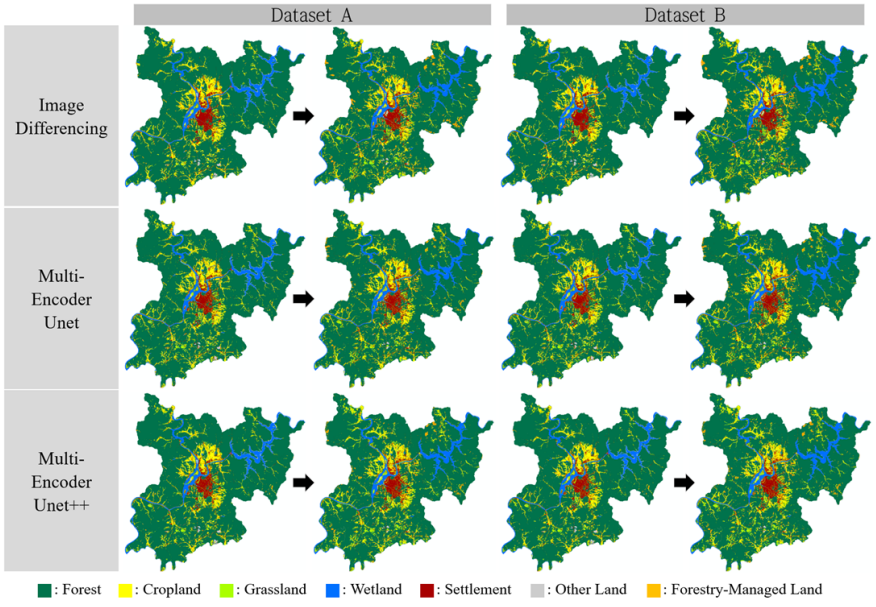

Fig. 3. Construction of time series land cover classification maps for detection of forest degradation.

Table 4. Evalation of consistency by deep learning models

Period	Accuracy	Image differencing		Multi-encoder Unet		Multi-encoder Unet++	
		Dataset A	Dataset B	Dataset A	Dataset B	Dataset A	Dataset B
The base year	OA	90.6%	91.0%	89.8%	90.2%	90.2%	90.2%
	Kappa	76.3%	77.1%	74.1%	74.5%	75.6%	75.7%
Final year	OA	90.6%	91.4%	89.2%	89.8%	90.0%	89.9%
	Kappa	77.2%	78.6%	73.0%	74.6%	75.0%	74.4%

Table 4). This finding is consistent with previous studies by Zheng et al. (2023) and Li et al. (2021). These similar results further support the effectiveness of integrating texture and terrain information in land cover classification tasks. Although there was only a marginal difference of 1-2% in classification accuracy among the deep learning models, it was found that the multi-encoder Unet++ was less cost-effective due to the longer training time required. Despite the Unet++ model's skip-connection structure incorporating multi-scale information, it did not significantly enhance performance with the time-series data used in this study. Therefore, future research should focus on improving feature extraction techniques, such as incorporating transformer modules, instead of solely enhancing the decoder structure.

Comparison of forest degradation detection consistency and analysis of misclassification characteristics across different deep learning models

It was observed that the accuracy of forest degradation detection exceeded 98% across all models when comparing the consistency between the forest degradation detection maps generated by different deep learning models and the label images of forest degradation, which covered the entire area of each county. Regardless of the dataset used, an accuracy of over 98% for forest degradation detection was achieved, with almost no difference observed among them. The image differencing technique based on Dataset B resulted in the highest accuracy in forest degradation detection, although the difference was negligible.

An instance was noted where forestry-managed lands were misclassified as grasslands or croplands during the final period. The classification accuracy of forestry-managed lands was approximately 70%, indicating the need for improved spatial information regarding forest management activities. Misclassifications mainly occurred at the outer boundaries of forests, likely due to positional errors of 1-2 pixels between satellite images and cadastral maps or time-series images. Such cases were observed to be distributed across the entire region without a specific pattern and could potentially be addressed through the application of filtering techniques in the future.

Conclusion

A study was conducted to compare three change detection techniques using time-series satellite imagery to assess forest degradation. Deep learning models were used for the analysis, and the results showed that the multi-encoder Unet model was the most effective in terms of both analysis time and accuracy. The multi-encoder model allowed baseline and final-year information to be input simultaneously, which made the analysis process more convenient. However, it was unclear whether the multi-encoder Unet++ model was more efficient than the image differencing technique in terms of analysis time or accuracy.

The study also found that incorporating texture or terrain information alongside spectral information improved the accurate classification of land cover categories. Moreover, the authors considered adding forestry-managed lands as an additional category, but this approach encountered limitations due to misclassifications of grassland or cropland as forestry-managed lands. Therefore, further investigation into diverse input information and model parameters is necessary for categories with similar spectral characteristics.

Acknowledgements

This research was funded by the Korea National Institute of Forest Science under project FM 0103-2021- 04-2023.

References

Cha SE, Won MS, Jang KC, Kim KM, Kim WK, Baek SI, Lim JB. 2022. Deep Learning-based Forest Fire Classification Evaluation for Application of CAS500-4. Korean J Remote Sens 38: 1273-1283.

Chen J, Lu Y, Yu Q, Luo X, Adeli E, Wang Y, Lu L, Yuille AL, Zhou Y. 2021. TransUNet: Transformers Make Strong Encoders for Medical Image Segmentation. arXiv doi: 10.48550/arXiv.2102.04306.

Cho KH, van Merrienboer B, Gulcehre C, Bahdanau D, Bougares F, Schwenk H, Bengio Y. 2014. Learning Phrase Representations using RNN Encoder-Decoder for Statistical Machine Translation. arXiv doi: 10.48550/arXiv.1406.1078.

Clausi DA. 2002. An analysis of co-occurrence texture statistics as a function of grey level quantization. Can J Remote Sens 28: 45-62.

Géron A. 2022. Hands-On Machine Learning with Scikit-Learn, Keras, and TensorFlow. 3rd ed. O'Reilly Media, Zurich.

Haralick RM, Shanmugam K, Dinstein I. 1973. Textural Features for Image Classification. IEEE Trans Syst Man Cybern 6: 610-621.

Huang MH, Rust RT. 2018. Artificial Intelligence in Service. J Serv Res 21: 155-172.

Kim ES, Won MS, Kim KM, Park JW, Lee JS. 2019. Forest Management Research using Optical Sensors and Remote Sensing Technologies. Korean J Remote Sens 35: 1031-1035.

Kingma DP, Ba J. 2014. Adam: A Method for Stochastic Optimization. arXiv doi: 10.48550/arXiv.1412.6980.

Korea Forest Service. 2024. K-Forest. https://www.forest.go.kr/kfsweb/cmm/fms/FileDown.do;jsessionid=ilhoHh5xod-laj9EjQFVng72ZmSquwRmeOHcfgEKOp6bvbLJ3J9FsuCkqyoYpAx6h.frswas01_servlet_engine5?atchFileId=FILE_000000020048405&fileSn=1&dwldHistYn=N&bbsId=BBSMSTR_1018. Accessed 15 Feb 2023.

Kross A, McNairn H, Lapen D, Sunohara M, Champagne C. 2015. Assessment of RapidEye vegetation indices for estimation of leaf area index and biomass in corn and soybean crops. Int J Appl Earth Observ Geoinf 34: 235-248.

Lee WK, Kim MI, Song CH, Lee SG, Cha SE, Kim GS. 2016. Application of Remote Sensing and Geographic Information System in Forest Sector. J Cadastre Land InformatiX 46: 27-42.

Li W, Li Y, Gong J, Feng Q, Zhou J, Sun J, Shi C, Hu W. 2021. Urban Water Extraction with UAV High-Resolution Remote Sensing Data Based on an Improved U-Net Model. Remote Sens 13: 3165.

Loshchilov I, Hutter F. 2018. Fixing Weight Decay Regularization in Adam. https://openreview.net/forum?id=rk6qdGgCZ. Accessed 15 Feb 2024.

Ministry of Land, Infrastructure and Transport. 2023. Cadastral Statistics. https://stat.molit.go.kr/portal/cate/statMetaView.do?hRsId=24. Accessed 15 Feb 2023.

Oktay O, Schlemper J, Folgoc LL, Lee M, Heinrich M, Misawa K, Mori K, McDonagh S, Hammerla NY, Kainz B, Glocker B, Rueckert D. 2018. Attention U-Net: Learning Where to Look for the Pancreas. arXiv doi: 10.48550/arXiv.1804.03999.

Park EB, Song CH, Ham BY, Kim JW, Lee JY, Choi SE, Lee WK. 2018. Comparison of Sampling and Wall-to-Wall Methodologies for Reporting the GHG Inventory of the LULUCF Sector in Korea. J Clim Chang Res 9: 385-398.

Ronneberger O, Fischer P, Brox T. 2015. U-Net: Convolutional Networks for Biomedical Image Segmentation. In: Medical Image Computing and Computer-Assisted Intervention - MICCAI 2015 (Navab N, Hornegger J, Wells W, Frangi A, eds). Springer, Cham, pp 234-241.

Rouhi R, Jafari M, Kasaei S, Keshavarzian P. 2015. Benign and malignant breast tumors classification based on region growing and CNN segmentation. Expert Syst Appl 42: 990-1002.

Rumelhart DE, Hinton GE, Williams RJ. 1986. Learning representations by back-propagating errors. Nature 323: 533-536.

Smith LN, Topin N. 2019. Super-convergence: very fast training of neural networks using large learning rates. SPIE 11006: 369-386.

Solórzano JV, Mas JF, Gao Y, Gallardo-Cruz JA. 2021. Land Use Land Cover Classification with U-Net: Advantages of Combining Sentinel-1 and Sentinel-2 Imagery. Remote Sens 13: 3600.

Son SH, Lee SH, Bae JG, Ryu MJ, Lee DI, Park SR, Seo DJ, Kim JS. 2022. Land-Cover-Change Detection with Aerial Orthoimagery Using SegNet-Based Semantic Segmentation in Namyangju City, South Korea. Sustainability 14: 12321.

Woo HS, Cho SW, Jung GH, Park JW. 2019. Precision Forestry Using Remote Sensing Techniques: Opportunities and Limitations of Remote Sensing Application in Forestry. Korean J Remote Sens 35: 1067-1082.

Zhang P, Ke Y, Zhang Z, Wang M, Li P, Zhang S. 2018. Urban Land Use and Land Cover Classification Using Novel Deep Learning Models Based on High Spatial Resolution Satellite Imagery. Sensors 18: 3717.

Zheng X, Han L, He G, Wang N, Wang G, Feng L. 2023. Semantic Segmentation Model for Wide-Area Coseismic Landslide Extraction Based on Embedded Multichannel Spectral–Topographic Feature Fusion: A Case Study of the Jiuzhaigou Ms7.0 Earthquake in Sichuan, China. Remote Sens 15: 1084.

Zhou Z, Rahman Siddiquee MM, Tajbakhsh N, Liang J. 2018. UNet++: A Nested U-Net Architecture for Medical Image Segmentation. In: Deep learning in medical image analysis and multimodal learning for clinical decision support (Stoyanov D, Taylor Z, Carneiro G, Syeda-Mahmood T, Martel A, Maier-Hein L, Tavares JMRS, Bradley A, Papa JP, Belagiannis V, Nascimento JC, Lu Z, Conjeti S, Moradi M, Greenspan H, Madabhushi A, eds). Springer, Cham, pp 3-11.